

# RIZE: Regularized Imitation Learning via Distributional Reinforcement Learning

Adib Karimi

Amirkabir University of Technology  
adibkarimi23@aut.ac.ir

Mohammad Mehdi Ebadzadeh

Amirkabir University of Technology  
ebadzadeh@aut.ac.ir

## Abstract

We introduce a novel Inverse Reinforcement Learning (IRL) approach that overcomes limitations of fixed reward assignments and constrained flexibility in implicit reward regularization. By extending the Maximum Entropy IRL framework with a squared temporal-difference (TD) regularizer and adaptive targets, dynamically adjusted during training, our method indirectly optimizes a reward function while incorporating reinforcement learning principles. Furthermore, we integrate distributional RL to capture richer return information. Our approach achieves state-of-the-art performance on challenging MuJoCo tasks, demonstrating expert-level results on the *Humanoid* task with only 3 *demonstrations*. Extensive experiments and ablation studies validate the effectiveness of our method, providing insights into adaptive targets and reward dynamics in imitation learning.<sup>1</sup>

## 1 Introduction

Inverse Reinforcement Learning (IRL) [Abbeel and Ng, 2004] is a foundational paradigm in artificial intelligence, enabling agents to acquire complex behaviors by observing expert demonstrations. This approach has catalyzed progress in diverse domains such as robotics [Osa et al., 2018], autonomous driving [Knox et al., 2023], and drug discovery [Ai et al., 2024]. By eliminating the need for explicitly defined reward functions, IRL provides a practical framework for training agents in environments where designing such functions is infeasible.

A prominent framework in IRL is Maximum Entropy (MaxEnt) IRL [Ziebart, 2010], which underpins many state-of-the-art (SOTA) IL methods. Prior works have combined MaxEnt IRL with adversarial training [Ho and Ermon, 2016, Fu et al., 2018] to minimize divergences between agent and expert distributions. However, these adversarial methods often suffer from instability during training. To address this, recent research has introduced implicit reward regularization, which indirectly represents rewards via Q-value functions by inverting the Bellman equation. For instance, IQ-Learn [Garg et al., 2021] unifies reward and policy representations using Q-functions with an  $L_2$ -norm regularization on rewards, while LSIQ [Al-Hafez et al., 2023] minimizes the chi-squared divergence between expert and mixture distributions, resulting in a squared temporal difference (TD) error objective analogous to SQIL [Reddy et al., 2020]. Despite its effectiveness, this method has limitations: LSIQ assigns fixed

---

<sup>1</sup>The code is available at <https://github.com/adibka/RIZE>.

rewards (e.g., +1 for expert samples and -1 for agent samples), which constrains flexibility by treating all tasks and state-action pairs uniformly, limiting performance and requiring additional gradient steps for convergence.

We present an extension of implicit reward regularization under the MaxEnt IRL framework through two methodological innovations: (1) **adaptive target rewards** ( $\lambda^{\pi_E}, \lambda^{\pi}$ ) that dynamically adjust during training to replace static targets, enabling context-sensitive alignment of expert and policy data, and (2) **distributional RL integration**, where value distributions  $Z^{\pi}(s, a)$  [Bellemare et al., 2017] are trained to capture richer return information while preserving theoretical consistency with Q-values, as the expectation of the value distribution is used for policy and value function optimization. By unifying adaptive target regularization with distributional insights [Zhou et al., 2023], our framework addresses prior rigidity in reward learning and empirically outperforms online IL baselines on MuJoCo benchmarks [Todorov et al., 2012], marking a novel integration of distributional RL into non-adversarial IRL.

Our contributions are as follow:

- We introduce adaptive target rewards for implicit reward regularization to enable dynamic adjustments during training.
- We leverage value distributions instead of classical Q-functions to capture richer insights from return distributions.
- We demonstrate the effectiveness of our approach through extensive experiments on MuJoCo tasks, providing detailed analyses of implicit rewards and adaptive target mechanisms.

## 2 Related Works

Imitation learning (IL) and inverse reinforcement learning (IRL) [Watson et al., 2023] are foundational paradigms for training agents to mimic expert behavior from demonstrations. Behavioral Cloning (BC) [Pomerleau, 1991], the simplest IL approach, treats imitation as a supervised learning problem by directly mapping states to expert actions. While computationally efficient, BC is prone to compounding errors [Ross and Bagnell, 2011] due to covariate shift during deployment. The Maximum Entropy IRL framework [Ziebart, 2010] addresses this limitation by probabilistically modeling expert behavior as reward maximization under an entropy regularization constraint, establishing a theoretical foundation for modern IRL methods.

The advent of adversarial training marked a pivotal shift in IL methodologies. Ho and Ermon [2016] introduced Generative Adversarial Imitation Learning (GAIL), which formulates imitation learning as a generative adversarial game [Goodfellow et al., 2014] where an agent learns a policy indistinguishable from the expert’s by minimizing the Jensen-Shannon divergence between their state-action distributions. This framework was generalized by Ghasemipour et al. [2019] in f-GAIL, which replaces the Jensen-Shannon divergence with arbitrary  $f$ -divergences to broaden applicability. Concurrently, Kostrikov et al. [2019] proposed Discriminator Actor-Critic (DAC), improving sample efficiency via off-policy updates and terminal-state reward modeling while mitigating reward bias.

Recent advances have shifted toward methods that bypass explicit reward function estimation.

Kostrikov et al. [2020] introduced ValueDICE, an offline IL method that leverages an inverse Bellman operator to avoid adversarial optimization. Similarly, Garg et al. [2021] developed IQ-Learn, which circumvents the challenges of MaxEnt IRL by optimizing implicit rewards derived directly from expert Q-values. A parallel research direction simplifies reward engineering by assigning fixed rewards to expert and agent samples. Reddy et al. [2020] pioneered this approach with Soft Q Imitation Learning (SQIL), which assigns binary rewards to transitions from expert and agent trajectories. Most recently, Al-Hafez et al. [2023] proposed Least Squares Inverse Q-Learning (LSIQ), enhancing regularization by minimizing chi-squared divergence between expert and mixture distributions while explicitly managing absorbing states through critic regularization. Our work builds on these foundations by integrating distributional RL [Dabney et al., 2018a] and introducing a squared TD regularizer with adaptive targets.

### 3 Background

#### 3.1 Preliminary

We consider a Markov Decision Process (MDP) [Puterman, 2014] to model policy learning in Reinforcement Learning (RL). The MDP framework is defined by the tuple  $\langle \mathcal{S}, \mathcal{A}, p_0, P, R, \gamma \rangle$ , where  $\mathcal{S}$  denotes the state space,  $\mathcal{A}$  the action space,  $p_0$  the initial state distribution,  $P : \mathcal{S} \times \mathcal{A} \times \mathcal{S} \rightarrow [0, 1]$  the transition kernel with  $P(\cdot | s, a)$  specifying the likelihood of transitioning from state  $s$  given action  $a$ ,  $R : \mathcal{S} \times \mathcal{A} \rightarrow \mathbb{R}$  the reward function, and  $\gamma \in [0, 1]$  the discount factor which tempers future rewards. A stationary policy  $\pi \in \Pi$  is characterized as a mapping from states  $s \in \mathcal{S}$  to distributions over actions  $a \in \mathcal{A}$ . The primary objective in RL [Sutton and Barto, 2018] is to maximize the expected sum of discounted rewards, expressed as  $\mathbb{E}_\pi [\sum_{t=0}^{\infty} \gamma^t R(s_t, a_t)]$ . Furthermore, the occupancy measure  $\rho_\pi(s, a)$  for a policy  $\pi \in \Pi$  is given by  $(1 - \gamma)\pi(a | s) \sum_{t=0}^{\infty} \gamma^t P(s_t = s | \pi)$ . The corresponding measure for an expert policy,  $\pi_E$ , is similarly denoted by  $\rho_E$ . In Imitation Learning (IL), it is posited that the expert policy  $\pi_E$  remains unknown, and access is restricted to a finite collection of expert demonstrations, represented as  $(s, a, s')$ .

#### 3.2 Distributional Reinforcement Learning

Maximum Entropy (MaxEnt) RL [Haarnoja et al., 2018] focuses on addressing the stochastic nature of action selection by maximizing the entropy of the policy, while Distributional RL [Bellemare et al., 2017] emphasizes capturing the inherent randomness in returns. Combining these perspectives, the distributional soft value function  $Z^\pi : \mathcal{S} \times \mathcal{A} \rightarrow \mathcal{Z}$  [Ma et al., 2020] for a policy  $\pi \in \Pi$  encapsulates uncertainty in both rewards and actions. It is formally defined as:

$$Z^\pi(s, a) = \sum_{t=0}^{\infty} \gamma^t [R(s_t, a_t) + \alpha \mathcal{H}(\pi(\cdot | s_t))], \quad (1)$$

where  $\mathcal{Z}$  represents the space of action-value distributions,  $\mathcal{H}(\pi) = \mathbb{E}_\pi[-\log \pi(a | s)]$  denotes the entropy of the policy, and  $\alpha > 0$  balances entropy with reward.

The distributional soft Bellman operator  $\mathcal{B}_D^\pi : \mathcal{Z} \rightarrow \mathcal{Z}$  for a given policy  $\pi$  is introduced as

$(\mathcal{B}_D^\pi Z)(s, a) \stackrel{D}{=} R(s, a) + \gamma[Z(s', a') - \alpha \log \pi(a' | s')]$ , where  $s' \sim P(\cdot | s, a)$ ,  $a' \sim \pi(\cdot | s')$ , and  $\stackrel{D}{=}$  signifies equality in distribution. Notably, this operator exhibits contraction properties under the p-Wasserstein metric, ensuring convergence to the optimal distributional value function.

A practical approach to approximating the value distribution  $Z$  involves modeling its quantile function  $F_Z^{-1}(\tau)$ , evaluated at specific quantile levels  $\tau \in [0, 1]$  [Dabney et al., 2018b]. The quantile function is defined as  $F_Z^{-1}(\tau) = \inf\{z \in \mathbb{R} : \tau \leq F_Z(z)\}$ , where  $F_Z(z) = \mathbb{P}(Z \leq z)$  is the cumulative distribution function of  $Z$ . For simplicity, we denote the quantile-based representation as  $Z_t^\pi(s, a) := F_Z^{-1}(\tau)$ . To discretize this representation, we define a sequence of quantile levels, denoted as  $\{\tau_i\}_{i=0, \dots, N-1}$ , where  $0 = \tau_0 < \dots < \tau_{N-1} = 1$ . These quantiles partition the unit interval into  $N$  fractions. Sampling uniformly from this interval  $\tau \sim U(0, 1)$ , we obtain an approximation of the value distribution  $Z_t^\pi(s, a)$ , which provides quantile values at these specified levels.

### 3.3 Inverse Reinforcement Learning

Given expert trajectory data, Maximum Entropy (MaxEnt) Inverse RL [Ziebart, 2010] aims to infer a reward function  $R(s, a)$  from the family  $\mathcal{R} = \mathbb{R}^{S \times A}$ . Instead of assuming a deterministic expert policy, this method optimizes for stochastic policies  $\pi \in \Pi$  that maximize  $R$  while matching expert behavior. Ho and Ermon [2016] extend this framework by introducing a convex reward regularizer  $\psi : \mathbb{R}^{S \times A} \rightarrow \bar{\mathbb{R}}$ , leading to the adversarial objective:

$$\max_{R \in \mathcal{R}} \min_{\pi \in \Pi} L(\pi, R) = \mathbb{E}_{\rho_E}[R(s, a)] - \mathbb{E}_{\rho_\pi}[R(s, a)] - \mathcal{H}(\pi) - \psi(R) \quad (2)$$

IQ-Learn [Garg et al., 2021] departs from adversarial training by implicitly representing rewards through Q-functions  $Q \in \Omega$  [Piot et al., 2014]. It leverages the inverse soft Bellman operator  $\mathcal{T}^\pi$ , defined as:

$$(\mathcal{T}^\pi Q)(s, a) = Q(s, a) - \gamma \mathbb{E}_{s' \sim P(\cdot | s, a), a' \sim \pi(\cdot | s')} [Q(s', a') - \alpha \log \pi(a' | s')] \quad (3)$$

For a fixed policy  $\pi$ ,  $\mathcal{T}^\pi$  is bijective, ensuring a one-to-one correspondence between Q-values and rewards:  $\mathcal{T}^\pi Q = R$  and  $Q = (\mathcal{T}^\pi)^{-1}R$ . This allows reframing the MaxEnt IRL objective in Q-policy space as  $\max_{Q \in \Omega} \min_{\pi \in \Pi} \mathcal{J}(\pi, Q)$ . IQ-Learn simplifies the problem by defining the implicit reward  $R_Q(s, a) = \mathcal{T}^\pi Q(s, a)$  and applying an L2 regularizer  $\psi(R_Q)$ . The final objective becomes:

$$\mathcal{J}(\pi, Q) = \mathbb{E}_{\rho_E}[R_Q(s, a)] - \mathbb{E}_{\rho_\pi}[R_Q(s, a)] - \mathcal{H}(\pi) - c (\mathbb{E}_{\rho_E}[R_Q^2] + \mathbb{E}_{\rho_\pi}[R_Q^2]). \quad (4)$$

## 4 Methodology

In this section, we present a systematic framework for developing our proposed approach. We begin by integrating Distributional RL with Imitation Learning (IL). Next, we introduce a novel regularization technique that enhances existing Implicit Reward methods through an adaptive reward mechanism. Finally, we propose our algorithm, which leverages the strengths of both Distributional RL and IL to achieve superior performance in complex environments.

## 4.1 Distributional Value Function

Our method diverges from traditional imitation learning by modeling value distributions as critics in an actor-critic framework [Zhou et al., 2023]. We propose that learning the full return distribution  $Z^\pi(s, a)$ —rather than point estimates like  $Q^\pi(s, a)$ —enables better decision-making in complex environments. By optimizing policies using the expectation of  $Z^\pi(s, a)$ , we derive a more robust learning signal. This robustness stems from explicitly capturing environmental stochasticity through distributional modeling, avoiding the limitations of Q-networks that collapse variability into deterministic estimates. In Distributional RL, the action-value function is defined as  $Q^\pi(s, a) = \mathbb{E}[Z^\pi(s, a)]$ , preserving the mathematical properties required by the IQ-Learn framework, ensuring theoretical consistency (see Lemma A.1 for more details).

## 4.2 Implicit Reward Regularization

In this section, we propose a novel regularizer for Inverse Reinforcement Learning (IRL) that refines existing implicit reward formulations [Garg et al., 2021]. We define the implicit reward as  $R_Q(s, a) = Q^\pi(s, a) - \gamma V^\pi(s')$ , where  $V^\pi(s') = Q^\pi(s', a') - \alpha \log \pi(a'|s')$ . Prior work often regularizes implicit rewards using  $L_2$ -norms, treating them as squared Temporal Difference (TD) errors between rewards and fixed targets [Reddy et al., 2020, Al-Hafez et al., 2023]. While adopting a similar squared TD framework [Mnih et al., 2015], we introduce adaptive targets  $\lambda^{\pi_E}$  (for expert policy  $\pi_E$ ) and  $\lambda^\pi$  (for imitation policy  $\pi$ ) to derive our convex regularizer  $\Gamma : \mathbb{R}^{S \times A} \rightarrow \bar{\mathbb{R}}$ :

$$\Gamma(R_Q, \lambda) = \mathbb{E}_{\rho_E} [(R_Q - \lambda^{\pi_E})^2] + \mathbb{E}_{\rho_\pi} [(R_Q - \lambda^\pi)^2]. \quad (5)$$

**Lemma 4.1.** *The implicit reward structure  $R_Q$  and regularizer  $\Gamma$  (Equation 5) guarantee:*

- **Bounded Rewards:**  $R_Q$  converges to a convex combination of adaptive targets  $\lambda^{\pi_E}$  and  $\lambda^\pi$ .
- **Temporal Consistency:** Ensures  $|Q(s, a) - \gamma Q(s', a')| \leq |\lambda| + |\epsilon| + \gamma\alpha |\log \pi(a'|s')|$ , where  $\epsilon$  is the optimization tolerance.

(Proof: Appendix A.)

This framework stabilizes learning by tethering rewards  $R_Q$  to adaptive targets that evolve with the policy, unlike static methods (e.g., LSIQ/SQIL) that use fixed rewards ( $\pm 1$ ). By co-optimizing  $R_Q$  and  $\lambda$ , we establish dynamic equilibrium—targets adapt to the current policy to avoid brittle regularization while maintaining bounded Q-values. The temporal consistency property ensures smooth value function updates, which directly translates to robust policy updates—reducing variance and improving the likelihood of convergence to the optimal policy. This dual adaptability distinguishes our approach from prior rigid regularization schemes.

## 4.3 Algorithm

We introduce **RIZE: Regularized Imitation Learning via Distributional Reinforcement Learning**, an algorithm enhancing implicit reward IRL through a convex regularizer inspired by TD error minimization. Unlike standard RL that uses environmental rewards, RIZE employs self-updating

adaptable targets, creating a somewhat reinforcement paradigm where rewards automatically align with their moving targets through regularization (see Algorithm 1).

### Critic Updates

Let  $Z_{\phi, \tau}^{\pi}(s, a)$  denote the return distribution and  $\pi_{\theta}(a|s)$  the policy. We compute Q-values as:

$$Q^{\pi}(s, a) = \sum_{i=0}^{N-1} (\tau_{i+1} - \tau_i) Z_{\phi, \tau_i}^{\pi}(s, a) \quad (6)$$

where  $\tau_i$  are quantile fractions and  $Z_{\phi, \tau_i}^{\pi}(s, a)$  represents quantile-specific return distributions.

The core objective integrates a squared-error regularizer  $\Gamma(R_Q, \lambda)$  (Equation 5) to stabilize target alignment:

$$\begin{aligned} \mathcal{L}(\pi, Q) = & \mathbb{E}_{\rho_E}[R_Q] - \mathbb{E}_{\rho_{\pi}}[R_Q] - \mathcal{H}(\pi) \\ & - c [\mathbb{E}_{\rho_E}[(R_Q - \lambda^{\tau_E})^2] + \mathbb{E}_{\rho_{\pi}}[(R_Q - \lambda^{\pi})^2]] \end{aligned} \quad (7)$$

where implicit rewards  $R_Q$  derive from:  $R_Q(s, a) = Q^{\pi}(s, a) - \gamma [Q^{\pi}(s', a') - \alpha \log \pi(a'|s')]$

### Adaptive Target Updates

Targets  $\lambda^{\tau_E}$  and  $\lambda^{\pi}$  self-update via the following objectives, creating a feedback loop where reward estimates continuously adapt to match their moving targets.

$$\min_{\lambda^{\tau_E}} \mathbb{E}_{\rho_E} [R_Q - \lambda^{\tau_E}]^2, \quad \min_{\lambda^{\pi}} \mathbb{E}_{\rho_{\pi}} [R_Q - \lambda^{\pi}]^2 \quad (8)$$

---

### Algorithm 1 Regularized Imitation Learning via Distributional Reinforcement Learning

---

1: **Initialize** value distribution  $Z_{\phi}$ , policy  $\pi_{\theta}$ , and target rewards  $\lambda^{\tau_E}, \lambda^{\pi}$

2: **for** step  $i$  in  $\{1, \dots, N\}$  **do**

3:   **Calculate**  $Q(s, a) = \mathbb{E}[Z_{\phi}(s, a)]$  using Equation 6

4:   **Update value**  $Z_{\phi}$  using objective from Equation 7

5:

$$\phi_{t+1} \leftarrow \phi_t - \beta_Q \nabla_{\phi} [-J(\phi)]$$

6:   **Update policy**  $\pi_{\theta}$  (like SAC)

7:

$$\theta_{t+1} \leftarrow \theta_t + \beta_{\pi} \nabla_{\theta} \mathbb{E}_{s \sim \mathcal{D}, a \sim \pi_{\theta}(\cdot|s)} [\min_{k=1,2} Q_k(s, a) - \alpha \log \pi_{\theta}(a|s)]$$

8:   **Update target rewards**  $\lambda^{\pi}$  and  $\lambda^{\tau_E}$  using objectives in 8

9:

$$\lambda_{t+1}^{\pi} \leftarrow \lambda_t^{\pi} - \beta_{\lambda} \nabla_{\lambda^{\pi}} \Gamma(R_Q, \lambda)$$

10:

$$\lambda_{t+1}^{\tau_E} \leftarrow \lambda_t^{\tau_E} - \beta_{\lambda} \nabla_{\lambda^{\tau_E}} \Gamma(R_Q, \lambda)$$

11: **end for**

---

## 5 Experiments

We evaluate our algorithm on four MuJoCo [Todorov et al., 2012] benchmarks (HalfCheetah-v2, Walker2d-v2, Ant-v2, Humanoid-v2) against state-of-the-art imitation learning methods: IQ-Learn [Garg et al., 2021], LSIQ [Al-Hafez et al., 2023], and SQIL [Reddy et al., 2020]. All experiments are conducted with five seeds for statistical significance [Henderson et al., 2018]. To assess sample efficiency, we test each method using three and ten expert trajectories. For ten trajectories, we retain baseline hyperparameters; for three trajectories (not reported in prior works), we adapt configurations from single-demonstration settings. IQ-Learn and LSIQ use their official implementations, while SQIL is evaluated using the LSIQ codebase. Results report mean performance across five seeds, with half a standard deviation to indicate uncertainty, and lines are smoothed for better readability. We normalize episode returns based on expert performance.

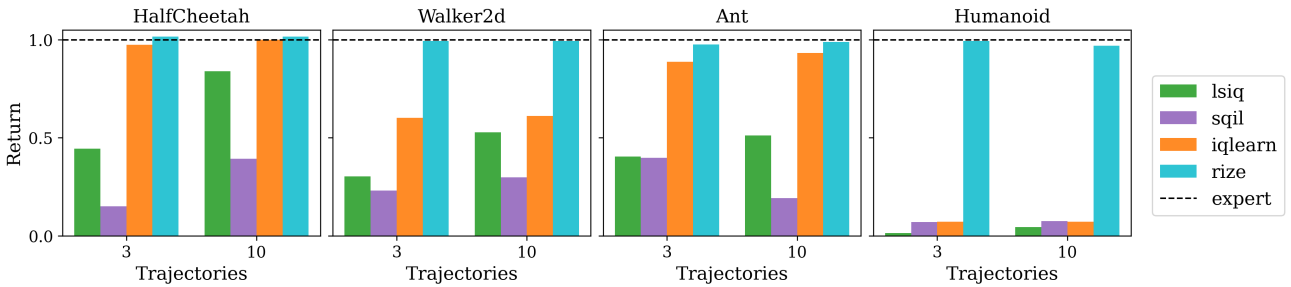


Figure 1: Normalized return of RIZE vs. online imitation learning baselines on Gym MuJoCo tasks. We depict the sorted top 25% episodic returns across five seeds to evaluate convergence to expert-level behavior. We evaluate with three and ten expert trajectories.

### 5.1 Main Results

Our method outperforms LSIQ and SQIL across tasks, with IQ-Learn as the only competitive baseline. Notably, in the most complex environment, Humanoid-v2, our approach is the sole method achieving expert-level performance, while all baselines fail (see Figure 1). This demonstrates our algorithm’s scalability to high-dimensional control problems. Additionally, our method shows superior sample efficiency, requiring fewer gradient steps to match expert performance compared to SOTA algorithms. These results highlight the robustness and efficiency of our approach in tackling complex tasks (see Figure 2).

### 5.2 Reward Dynamics Analysis

Our implicit reward regularizer  $\Gamma(R_Q, \lambda)$  (Equation 5), ensures proximity between the learned  $R_Q$  and target rewards  $\lambda$ . As illustrated in Figure 3, when provided with sufficient expert trajectories (ten demonstrations), the rewards for both the expert and the policy stabilize around consistent values, as observed in environments like HalfCheetah and Ant. While our method is not Adversarial IL, it extends MaxEnt IRL principles. This alignment is evident as the policy increasingly mirrors expert behavior, causing the discriminator to converge and provide similar reward signals for both the expert and policy samples. This convergence reflects an equilibrium between policy optimization and reward learning, demonstrating the stability and effectiveness of our approach.

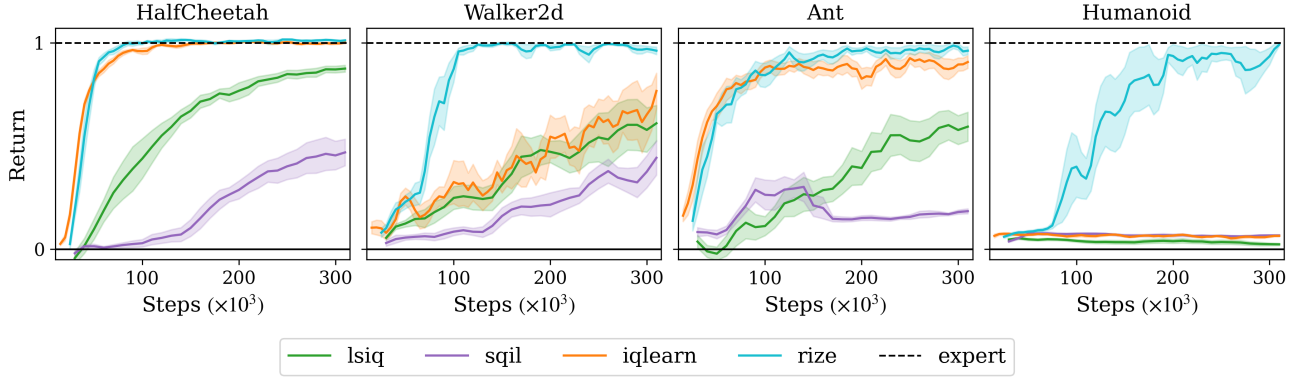


Figure 2: Normalized return of RIZE vs. online imitation learning baselines on Gym MuJoCo tasks. We use 10 expert trajectories for all tasks.

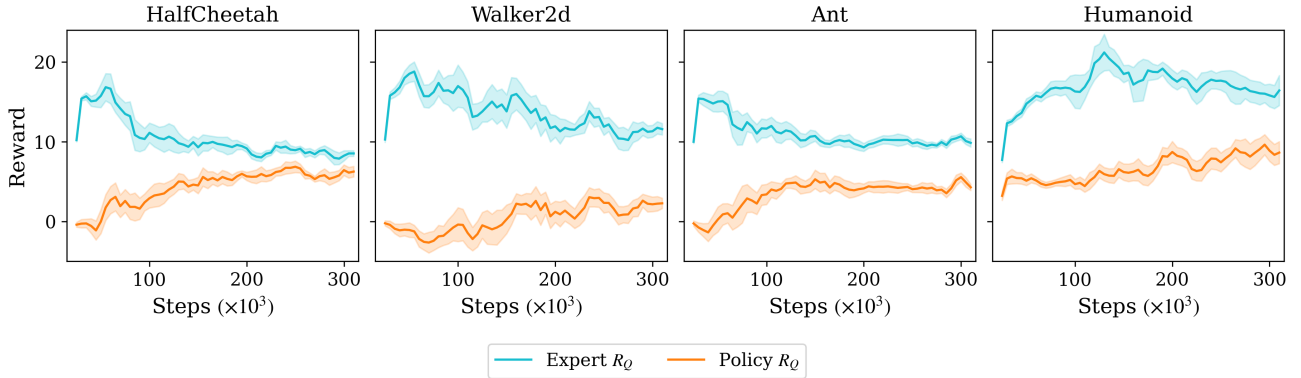


Figure 3: Implicit reward curves for expert and policy samples on Gym MuJoCo tasks. We use 10 expert trajectories for all tasks.

### 5.3 Ablation: Regularization Strategies

We investigate the effect of squared TD error regularization on the Ant-v2 task using three distinct formulations: *Expert-focused TD*:  $\mathbb{E}_{\rho_E}[R_Q - \lambda^{\pi_E}]^2 + \mathbb{E}_{\rho_\pi}[R_Q]^2$ , *Policy-focused TD*:  $\mathbb{E}_{\rho_E}[R_Q]^2 + \mathbb{E}_{\rho_\pi}[R_Q - \lambda^{\pi}]^2$ , *Baseline L2*:  $\mathbb{E}_{\rho_E}[R_Q]^2 + \mathbb{E}_{\rho_\pi}[R_Q]^2$ .



Our results in Figure 4 demonstrate that applying squared TD regularization to both expert and policy samples improves robustness. While the expert-focused TD formulation outperforms the policy-focused variant, neither consistently achieves expert-level behavior. Over time, both exhibit gradual performance degradation, underscoring the challenges of maintaining stable imitation. This highlights the need for more refined regularization strategies to ensure consistent and reliable learning in imitation learning.

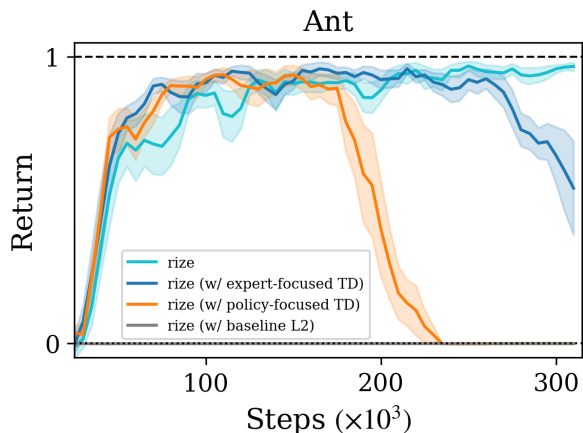


Figure 4: Ablation study on the effect of various regularization strategies on the Ant-v2 task, evaluated using three demonstrations. Turquoise represents RIZE using the convex regularizer  $\Gamma$ .

## 6 Conclusion

We present a novel IRL framework that overcomes the rigidity of fixed reward mechanisms through dynamic reward adaptation via context-sensitive regularization and probabilistic return estimation with distributional RL. By introducing adaptive target rewards that evolve during training—replacing static assignments—our method enables nuanced alignment of expert and agent trajectories, while value distribution integration captures richer return dynamics without sacrificing theoretical consistency. Empirical evaluations on MuJoCo benchmarks demonstrate state-of-the-art performance, achieving expert-level proficiency on the *Humanoid* task with only *three demonstrations*, alongside ablation studies confirming the necessity of applying our regularization mechanism. This work advances imitation learning by unifying flexible reward learning with probabilistic return representations, offering a scalable, sample-efficient paradigm for complex decision making. Future directions include extending these principles to offline IL and risk-sensitive robotics, where adaptive rewards and uncertainty-aware distributions could further enhance robustness and generalization.

## References

- P. Abbeel and A. Y. Ng. Apprenticeship learning via inverse reinforcement learning. In *International Conference on Machine Learning*, 2004.
- Cheng Ai, Hong Yang, Xinyu Liu, Ruijie Dong, Ying Ding, and Fei Guo. Mtmol-gpt: De novo multi-target molecular generation with transformer-based generative adversarial imitation learning. *PLoS Computational Biology*, 20(6):e1012229, 2024. doi: 10.1371/journal.pcbi.1012229. URL <https://doi.org/10.1371/journal.pcbi.1012229>.
- Firas Al-Hafez, Davide Tateo, Oleg Arenz, Guoping Zhao, and Jan Peters. LS-IQ: Implicit reward regularization for inverse reinforcement learning. In *The Eleventh International Conference on Learning Representations*, 2023. URL <https://openreview.net/forum?id=o3Q4m8jg4BR>.
- Marc G. Bellemare, Will Dabney, and Rémi Munos. A distributional perspective on reinforcement learning. In *International Conference on Machine Learning*, 2017. URL <https://api.semanticscholar.org/CorpusID:966543>.
- Greg Brockman, Vicki Cheung, Ludwig Pettersson, Jonas Schneider, John Schulman, Jie Tang, and Wojciech Zaremba. OpenAI Gym. *arXiv preprint arXiv:1606.01540*, 2016.
- Will Dabney, Georg Ostrovski, David Silver, and Remi Munos. Implicit quantile networks for distributional reinforcement learning. In *Proceedings of the 35th International Conference on Machine Learning*, Proceedings of Machine Learning Research, pages 1096–1105. PMLR, 2018a.
- Will Dabney, Mark Rowland, Marc G. Bellemare, and Remi Munos. Distributional reinforcement learning with quantile regression. In *Proceedings of the Thirty-Second AAAI Conference on Artificial Intelligence and Thirtieth Innovative Applications of Artificial Intelligence Conference and Eighth AAAI Symposium on Educational Advances in Artificial Intelligence*, AAAI’18/IAAI’18/EAAI’18. AAAI Press, 2018b. ISBN 978-1-57735-800-8.
- Justin Fu, Katie Luo, and Sergey Levine. Learning robust rewards with adversarial inverse reinforcement learning. In *International Conference on Learning Representations*, 2018.
- Divyansh Garg, Shuvam Chakraborty, Chris Cundy, Jiaming Song, and Stefano Ermon. Iq-learn: Inverse soft-q learning for imitation. In *Advances in Neural Information Processing Systems*, volume 34, 2021.
- Seyed Kamyar Seyed Ghasemipour, Richard Zemel, and Shixiang Gu. A divergence minimization perspective on imitation learning methods. In *Conference on Robot Learning*, 2019.
- Ian J Goodfellow, Jean Pouget-Abadie, Mehdi Mirza, Bing Xu, David Warde-Farley, Sherjil Ozair, Aaron Courville, and Yoshua Bengio. Generative adversarial networks. In *Advances in Neural Information Processing Systems*, volume 27, 2014.
- Tuomas Haarnoja, Aurick Zhou, Pieter Abbeel, and Sergey Levine. Soft actor-critic: Off-policy maximum entropy deep reinforcement learning with a stochastic actor. In *International Conference on Machine Learning*, 2018.

- Peter Henderson, Riashat Islam, Philip Bachman, Joelle Pineau, Doina Precup, and David Meger. Deep reinforcement learning that matters. In *Proceedings of the Thirty-Second AAAI Conference on Artificial Intelligence and Thirtieth Innovative Applications of Artificial Intelligence Conference and Eighth AAAI Symposium on Educational Advances in Artificial Intelligence, AAAI'18/IAAI'18/EAAI'18*. AAAI Press, 2018. ISBN 978-1-57735-800-8.
- Jonathan Ho and Stefano Ermon. Generative adversarial imitation learning. In *Advances in Neural Information Processing Systems*, volume 29, 2016.
- W. Bradley Knox, Alessandro Allievi, Holger Banzhaf, Felix Schmitt, and Peter Stone. Reward (mis)design for autonomous driving. *Artif. Intell.*, 316(C), March 2023. ISSN 0004-3702. doi: 10.1016/j.artint.2022.103829. URL <https://doi.org/10.1016/j.artint.2022.103829>.
- Ilya Kostrikov, Kumar Krishna Agrawal, Debidatta Dwibedi, Sergey Levine, and Jonathan Tompson. Discriminator-actor-critic: Addressing sample inefficiency and reward bias in adversarial imitation learning. In *International Conference on Learning Representations*, 2019.
- Ilya Kostrikov, Ofir Nachum, and Jonathan Tompson. Imitation learning via off-policy distribution matching. In *International Conference on Learning Representations*, 2020.
- Xiaoteng Ma, Qiyuan Zhang, Li Xia, Zhengyuan Zhou, Jun Yang, and Qianchuan Zhao. Dsac: Distributional soft actor critic for risk-sensitive reinforcement learning. *arXiv*, 2020.
- Volodymyr Mnih, Koray Kavukcuoglu, David Silver, Alex Graves, Ioannis Antonoglou, Daan Wierstra, and Martin Riedmiller. Human-level control through deep reinforcement learning. *Nature*, 518 (7540):529–533, 2015.
- Takayuki Osa, Joni Pajarinen, Gerhard Neumann, J. Andrew Bagnell, Pieter Abbeel, and Jan Peters. An algorithmic perspective on imitation learning. *Foundations and Trends in Robotics*, 2018.
- B. Piot, M. Geist, and O. Pietquin. Boosted and Reward-regularized Classification for Apprenticeship Learning. In *Proceedings of the International Conference on Autonomous Agents and Multiagent Systems (AAMAS)*, 2014.
- D. A. Pomerleau. Efficient training of artificial neural networks for autonomous navigation. *Neural Computation*, 3(1):88–97, 1991.
- Martin L. Puterman. *Markov Decision Processes: Discrete Stochastic Dynamic Programming*. John Wiley & Sons, 2014.
- Siddharth Reddy, Anca D Dragan, and Sergey Levine. Sqil: Imitation learning via reinforcement learning with sparse rewards. In *International Conference on Learning Representations*, 2020.
- Stéphane Ross and J. Andrew Bagnell. A reduction of imitation learning and structured prediction to no-regret online learning. In *International Conference on Artificial Intelligence and Statistics*, 2011.
- Richard S. Sutton and Andrew G. Barto. *Reinforcement Learning: An Introduction*. The MIT Press, Cambridge, Massachusetts; London, England, second edition, 2018.

- E. Todorov, T. Erez, and Y. Tassa. MuJoCo: A physics engine for model-based control. In *2012 IEEE/RSJ International Conference on Intelligent Robots and Systems*, pages 5026–5033, 2012.
- Joe Watson, Sandy Huang, and Nicolas Heess. Coherent soft imitation learning. In *Thirty-seventh Conference on Neural Information Processing Systems*, 2023. URL <https://openreview.net/forum?id=kCCD8d2aEu>.
- Y. Zhou, M. Lu, X. Liu, Z. Che, Z. Xu, J. Tang, and Y Zhang. Distributional generative adversarial imitation learning with reproducing kernel generalization. *Neural Networks*, 165, 2023.
- Brian D Ziebart. *Modeling purposeful adaptive behavior with the principle of maximum causal entropy*. PhD thesis, University of Washington, 2010.

## A Proofs

**Lemma A.1.** Consider an MDP with discount factor  $\gamma \in [0, 1)$  and rewards bounded by some constant  $C > 0$  such that  $|R(s, a)| \leq C$ . Define the return distribution as

$$Z(s, a) = \sum_{t=0}^{\infty} \gamma^t R(s_t, a_t),$$

where the trajectory  $\{(s_t, a_t)\}$  is generated by following policy  $\pi$  under dynamics  $\mathcal{P}$ . Then the classical action-value function is given by

$$Q^\pi(s, a) = \mathbb{E}_{\pi, \mathcal{P}}[Z(s, a)].$$

Moreover, if we approximate  $Z(s, a)$  by a learned distribution  $Z_\theta(s, a)$  with expectation  $\tilde{Q}(s, a) = \mathbb{E}[Z_\theta(s, a)]$ , then under the conditions of the Dominated Convergence Theorem (DCT),  $\tilde{Q}(s, a)$  converges to  $Q^\pi(s, a)$ .

*Proof of Lemma A.1.*

**Existence of the Expectation:** Since the rewards are bounded, we have  $|R(s_t, a_t)| \leq C$ , and the discounted series satisfies

$$\mathbb{E} \left[ \sum_{t=0}^{\infty} \gamma^t |R(s_t, a_t)| \right] \leq \sum_{t=0}^{\infty} \gamma^t C = \frac{C}{1-\gamma} < \infty.$$

This absolute convergence allows us to apply DCT:

$$\mathbb{E}[Z(s, a)] = \mathbb{E} \left[ \sum_{t=0}^{\infty} \gamma^t R(s_t, a_t) \right] = \sum_{t=0}^{\infty} \gamma^t \mathbb{E}[R(s_t, a_t)].$$

**Equivalence to Q-value:** By definition,

$$Q^\pi(s, a) = \mathbb{E}_{\pi, \mathcal{P}} \left[ \sum_{t=0}^{\infty} \gamma^t R(s_t, a_t) \right] = \mathbb{E}[Z(s, a)].$$

**Convergence of the Learned Distribution:** In distributional reinforcement learning, if we represent the return distribution using  $Z_\theta(s, a)$ , then its mean is given by

$$\tilde{Q}(s, a) = \mathbb{E}[Z_\theta(s, a)].$$

Under DCT conditions, we have

$$\tilde{Q}(s, a) \rightarrow Q^\pi(s, a).$$

□

*Proof of Lemma 4.1.*

### 1. Bounded Rewards

The expert and policy reward targets  $\lambda^{\pi_E}, \lambda^\pi$  are learned via:

$$\lambda^{\pi_E} \leftarrow \mathbb{E}_{\rho_E}[R_Q], \quad \lambda^\pi \leftarrow \mathbb{E}_{\rho_\pi}[R_Q].$$

This ensures  $\lambda^{\pi_E}$  and  $\lambda^\pi$  track the empirical mean of  $R_Q$ .

Fixing  $\lambda^{\pi_E}$  and  $\lambda^\pi$ , solving  $\nabla_{R_Q} \Gamma = 0$  yields:

$$R_Q = \frac{\rho_E \lambda^{\pi_E} + \rho_\pi \lambda^\pi}{\rho_E + \rho_\pi},$$

This is a convex combination of  $\lambda^{\pi_E}$  and  $\lambda^\pi$ . Since  $\lambda^{\pi_E}, \lambda^\pi$  are empirical means,  $|R_Q| \leq \max(|\lambda^{\pi_E}|, |\lambda^\pi|)$ , ensuring boundedness.

### 2. Temporal Consistency

The reward  $R_Q$  (for either expert or policy samples) is defined via the soft Q-function:

$$R_Q = Q(s, a) - \gamma \mathbb{E}_{s'} [Q(s', a') - \alpha \log \pi(a'|s')].$$

Rearranging gives:

$$Q(s, a) = R_Q + \gamma \mathbb{E}_{s'} [Q(s', a') - \alpha \log \pi(a'|s')] + \epsilon,$$

where  $\epsilon$  is the Bellman optimization error (due to approximation or finite samples). Substituting  $R_Q = \lambda$ :

$$Q(s, a) - \gamma Q(s', a') = \lambda + \epsilon - \gamma \alpha \log \pi(a'|s').$$

Taking absolute values:

$$|Q(s, a) - \gamma Q(s', a')| \leq |\lambda| + |\epsilon| + \gamma \alpha |\log \pi(a'|s')|.$$

This bounds successive Q-values, ensuring temporal consistency.

### Conclusion.

The adaptive regularizer  $\Gamma$  (Equation 5) enforces bounded rewards via convex combinations of empirical targets and ensures temporal consistency through entropy-regularized Q-value recursion. Both properties stabilize learning by preventing divergence.  $\square$

## B Experiments

### B.1 MuJoCo Control Suite

We evaluate our imitation learning approach, **RIZE**, on four benchmark Gym [Brockman et al., 2016] MuJoCo [Todorov et al., 2012] environments: *HalfCheetah-v2*, *Walker2d-v2*, *Ant-v2*, and *Humanoid-v2*. Expert trajectories are generated using a pretrained Soft Actor-Critic (SAC) [Haarnoja et al., 2018] agent, with each trajectory consisting of 1,000 state-action transitions. To facilitate performance comparisons, episode returns are normalized relative to expert performance: *HalfCheetah* (5100), *Walker2d* (5200), *Ant* (4700), and *Humanoid* (5300).

### B.2 Implementation Details

Our architecture integrates components from **Distributional SAC (DSAC)**<sup>2</sup> [Ma et al., 2020] and **IQ-Learn**<sup>3</sup> [Garg et al., 2021], with hyperparameters tuned through systematic search and ablation studies. Key configurations for experiments involving three demonstrations are summarized in Table 1, while Table 2 provides settings for scenarios with ten demonstrations. Our implementation can be found at <https://github.com/adibka/RIZE>.

**Distributional SAC Components:** The critic network is implemented as a three-layer multilayer perceptron (MLP) with 256 units per layer, trained using a learning rate of  $3 \times 10^{-4}$ . The policy network is a four-layer MLP, also with 256 units per layer. Environment-specific learning rates are applied:  $1 \times 10^{-5}$  for the *Humanoid* environment and  $5 \times 10^{-5}$  for all others. To enhance training stability, we employ a target policy—a delayed version of the online policy—and sample next-state actions from this module. For value distribution training  $Z_{\phi, \tau}^{\pi}$ , we adopt the Implicit Quantile Networks (IQN) [Dabney et al., 2018a] approach by sampling quantile fractions  $\tau$  uniformly from  $\mathcal{U}(0, 1)$ . Additionally, dual critic networks with delayed updates are used, which empirically improve training stability.

**IQ-Learn Adaptations:** Key adaptations from IQ-Learn include adjustments to the regularizer coefficient  $c$  and entropy coefficient  $\alpha$ . Specifically, for the regularizer coefficient  $c$ , we find that  $c = 0.5$  yields robust performance on the *Humanoid* task, while  $c = 0.1$  works better for other tasks. For the entropy coefficient  $\alpha$ , smaller values lead to more stable training. Unlike RL, where exploration is crucial, imitation learning relies less on entropy due to the availability of expert data. Across all tasks, we set initial target reward parameters as  $\lambda^{\tau_E} = 10$  and  $\lambda^{\tau} = 5$ . Furthermore, we observe that lower learning rates for target rewards improve overall learning performance.

Previous implicit reward methods such as IQLearn, ValueDICE, and LSIQ<sup>4</sup> have employed distinct modifications to the loss function. In our setup, two main loss variants are defined:

---

<sup>2</sup><https://github.com/xtma/dsac>

<sup>3</sup><https://github.com/Div99/IQ-Learn>

<sup>4</sup><https://github.com/robfirmas/ls-iq/tree/main>

1. **Value loss:**

$$\mathcal{L}(\pi, Q) = \mathbb{E}_{\rho_E}[Q^\pi(s, a) - \gamma V^\pi(s')] - \mathbb{E}_\rho[V^\pi(s) - \gamma V^\pi(s')] - c\Gamma(R_Q, \lambda) \quad (9)$$

2. **v0 loss:**

$$\mathcal{L}(\pi, Q) = \mathbb{E}_{\rho_E}[Q^\pi(s, a) - \gamma V^\pi(s')] - (1 - \gamma)\mathbb{E}_{p_0}[V^\pi(s_0)] - c\Gamma(R_Q, \lambda) \quad (10)$$

Here,  $\rho$  is a mixture distribution,  $p_0$  denotes the initial distribution,  $R_Q(s, a)$  is the implicit reward defined as  $R_Q(s, a) = Q^\pi(s, a) - \gamma V^\pi(s')$ , the state-value function is given by  $V^\pi(s') = Q^\pi(s', a') - \alpha \log \pi(a'|s')$ , and lastly, our convex regularizer is expressed as  $\Gamma(R_Q, \lambda) = \mathbb{E}_{\rho_E}[(R_Q - \lambda^{\pi_E})^2] + \mathbb{E}_{\rho_\pi}[(R_Q - \lambda^\pi)^2]$ .

The choice between *v0* or *value* loss variants depends on environment complexity: we find that for a complex task like *Humanoid-v2*, the *v0* variant demonstrates greater robustness. And, for simpler tasks such as *HalfCheetah-v2*, *Walker2d-v2*, and *Ant-v2*, the *value* variant performs better.

Table 1: Three Demonstrations Hyperparameters

Environment	$\alpha$	$c$	$\text{lr } \pi$	$\lambda^{\pi_E}$	$\text{lr } \lambda^{\pi_E}$	$\lambda^\pi$	$\text{lr } \lambda^{\pi_E}$
Ant-v2	0.05	0.1	$5 \times 10^{-5}$	10	$1 \times 10^{-4}$	5	$1 \times 10^{-5}$
HalfCheetah-v2	0.05	0.1	$5 \times 10^{-5}$	10	$1 \times 10^{-4}$	5	$1 \times 10^{-5}$
Walker2d-v2	0.05	0.1	$5 \times 10^{-5}$	10	$1 \times 10^{-4}$	5	$1 \times 10^{-5}$
Humanoid-v2	0.05	0.5	$1 \times 10^{-5}$	10	$1 \times 10^{-4}$	5	$5 \times 10^{-5}$

Table 2: 10 Demonstrations Hyperparameters

Environment	$\alpha$	$c$	$\text{lr } \pi$	$\lambda^{\pi_E}$	$\text{lr } \lambda^{\pi_E}$	$\lambda^\pi$	$\text{lr } \lambda^{\pi_E}$
Ant-v2	0.1	0.1	$5 \times 10^{-5}$	10	$1 \times 10^{-4}$	5	$1 \times 10^{-4}$
HalfCheetah-v2	0.1	0.1	$5 \times 10^{-5}$	10	$1 \times 10^{-4}$	5	$1 \times 10^{-4}$
Walker2d-v2	0.1	0.1	$5 \times 10^{-5}$	10	$1 \times 10^{-4}$	5	$1 \times 10^{-4}$
Humanoid-v2	0.1	0.5	$1 \times 10^{-5}$	10	$1 \times 10^{-4}$	5	$1 \times 10^{-5}$

### B.3 Extended Main Results

In this section, we showcase the performance of our method, RIZE, using both ten and three expert demonstrations. RIZE outshines LSIQ and SQIL in various tasks, with IQ-Learn as its only competitor. Remarkably, it reaches expert-level performance in the challenging Humanoid-v2 environment with just three trajectories, proving its scalability. Plus, it requires fewer training steps than other algorithms, emphasizing its efficiency and robustness in complex situations. Our findings demonstrate that using fewer expert samples does not negatively impact our imitation learning approach (see Figure 5).

### B.4 Extended Recovered Rewards

Here, we investigate the implicit reward dynamics of our method using both three and ten expert demonstrations. As illustrated in Figure 6, with ample expert trajectories (n=10), the rewards for both



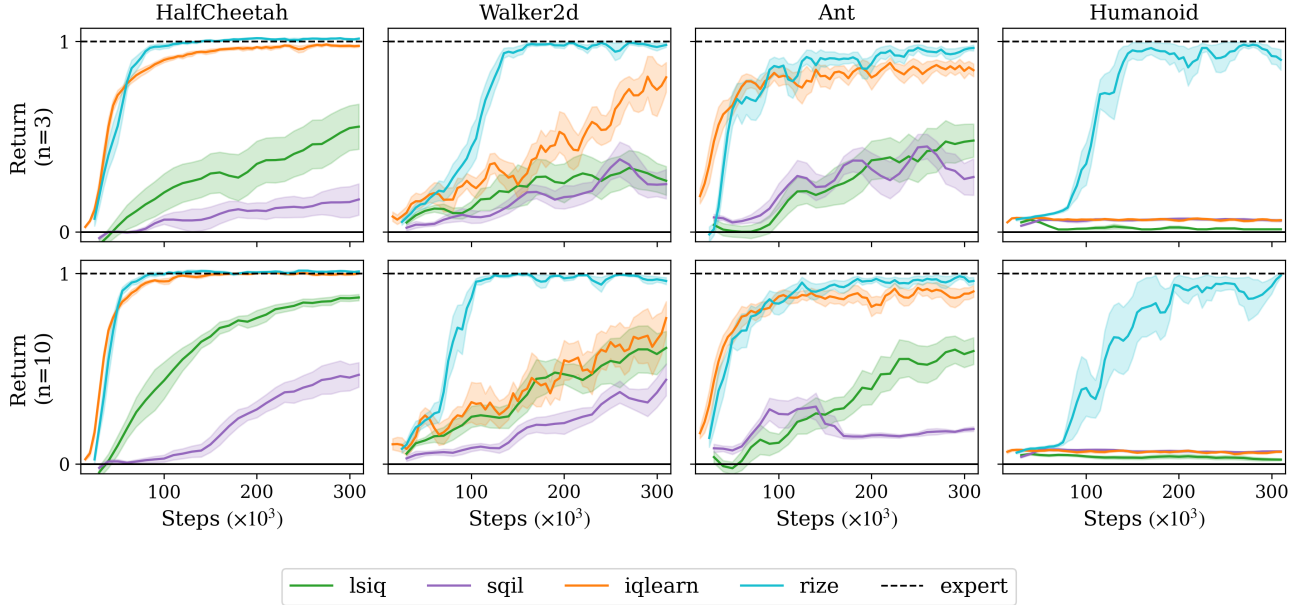


Figure 5: Normalized return of RIZE vs. online imitation learning baselines on Gym MuJoCo tasks.  $n$  denotes the number of expert trajectories.

the expert and the policy stabilize to consistent values across most environments. Notably, even with a three demonstrations, which presents a significant learning challenge, rewards still converge to similar values in tasks such as HalfCheetah and Humanoid.

Our implicit reward regularization term,  $\Gamma(R_Q, \lambda)$ , ensures the learned rewards stay close to the target rewards. Looking at Figure X, you can see that optimizing  $\lambda^{\pi_E}$  and  $\lambda^\pi$  using Equations X effectively bounds both the implicit and target rewards, boosting overall stability. Interestingly, for certain tasks like HalfCheetah-v2, Walker2d-v2, and Ant-v2,  $\lambda^\pi$  doesn't change much. This is because we deliberately used smaller learning rates, which proved crucial for maintaining training stability.

## B.5 Hyperparameter Fine-Tuning

We present our analysis and comparison of important hyperparameters utilized in our algorithm. As before, all experiments use five seeds, and we show mean and half a standard deviation of all the seeds. As a challenging task among MuJoCo environments, we only experiment with Ant-v2.

### Target Reward $\lambda$

Selecting appropriate initial values and learning rates for the automatic fine-tuning of  $\lambda^{\pi_E}$  and  $\lambda^\pi$  is critical in our approach. First, we observe that a suitable learning rate is essential for the stable training of our imitation learning agent, as illustrated in Figure 8a. Our findings indicate that  $\lambda^\pi$  must be optimized very slowly; using larger learning rates can destabilize training and hinder progress. In contrast,  $\lambda^{\pi_E}$  demonstrates greater resilience when optimized with higher learning rates. Additionally,  $\lambda^{\pi_E}$  remains robust even with varying initial values. However, as shown in Figure 8b, failing to select an appropriate initial value for  $\lambda^\pi$  can negatively impact learning. Overall, Figures 8a and 8b highlight the need for careful selection of both the learning rate and initial value when optimizing  $\lambda^\pi$ ,

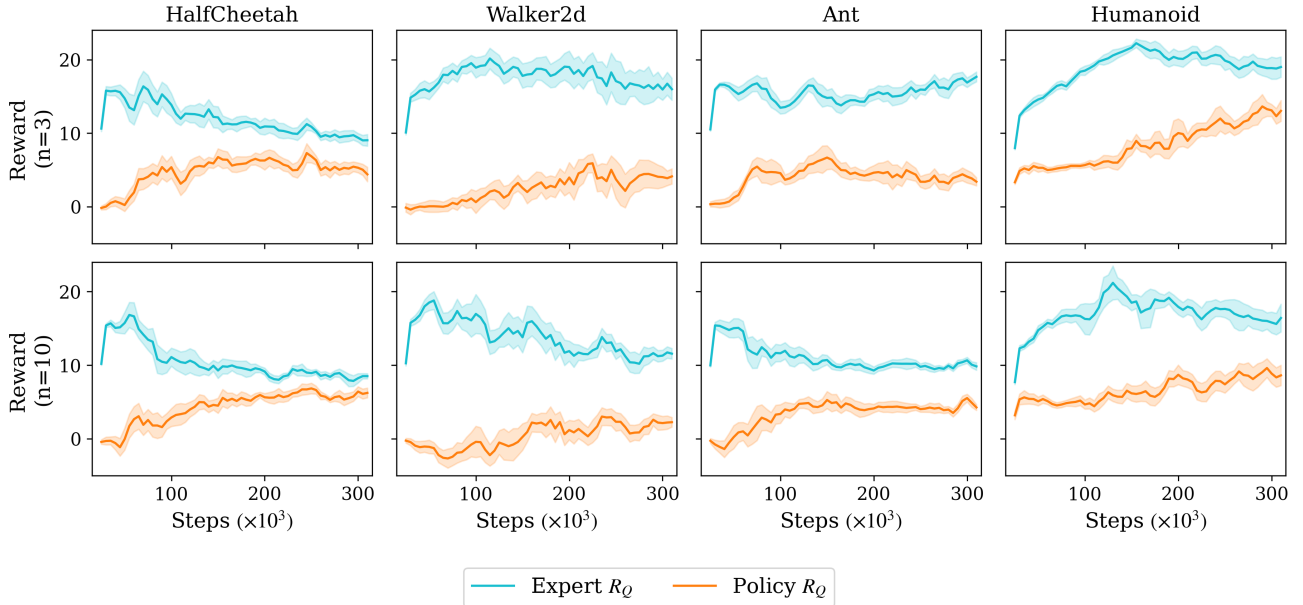


Figure 6: Implicit reward curves for expert and policy samples on Gym MuJoCo tasks.  $n$  represents the number of expert demonstrations.

while  $\lambda^{\pi_E}$  exhibits considerable robustness in this regard.

### Regularization Coefficient $C$

Our experiments on the regularizer coefficient,  $C$ , reveal that smaller values of  $C$  encourage expert-like performance, while larger values overly constrain rewards and targets, limiting learning. This finding highlights the critical role of selecting an appropriate  $C$ , as it directly impacts the balance between learning from expert data and regularization: higher values prioritize regularization at the cost of learning, whereas smaller values favor learning but reduce regularization (see Figure 9).

### Entropy Coefficient $\alpha$

We observe that the entropy coefficient is a crucial hyperparameter in inverse reinforcement learning (IRL) problems. As shown in Figure 10, IRL methods typically require small values for  $\alpha$ , a point previously noted by Reference X. With expert demonstrations available, an imitation learning (IL) policy does not need to explore for optimal actions, as these are provided by the demonstrations. Consequently, higher values of  $\alpha$  can lead to training instability, ultimately resulting in policy collapse.

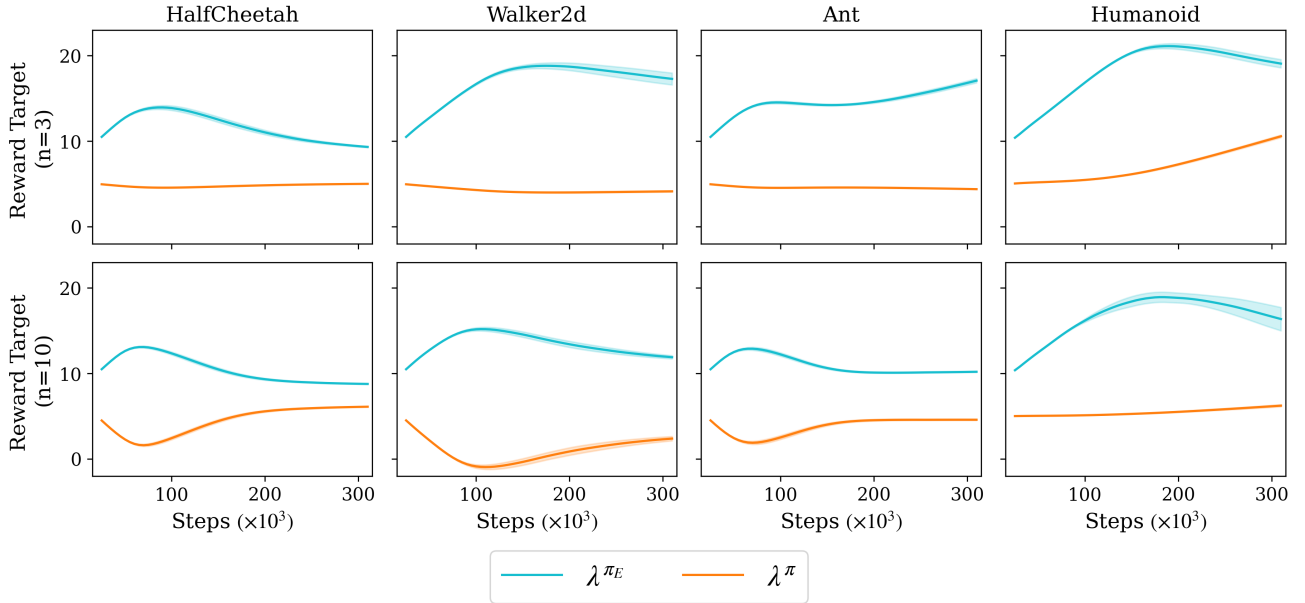


Figure 7: Target reward values for expert ( $\lambda^{\pi_E}$ ) and policy ( $\lambda^\pi$ ) on Gym MuJoCo tasks.  $n$  represents the number of expert demonstrations.

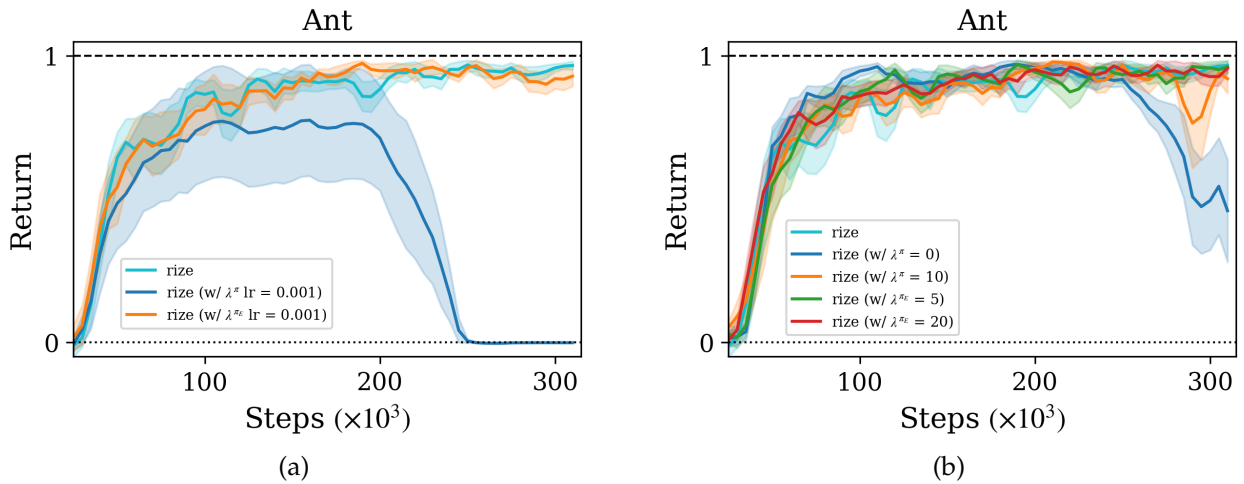


Figure 8: Fine-tuning of target parameters. (a) Turquoise represents our method’s primary result with learning rates of  $1e^{-4}$  for  $\lambda^{\pi_E}$  and  $1e^{-5}$  for  $\lambda^\pi$ . Orange and blue lines indicate higher learning rates (e.g., 0.001) for  $\lambda^{\pi_E}$  and  $\lambda^\pi$ , respectively. (b) Turquoise shows the main result with initial values of 10 for  $\lambda^{\pi_E}$  and 5 for  $\lambda^\pi$ , while other lines explore different starting values. Only one parameter is varied at a time, and three trajectories are used throughout the analysis.

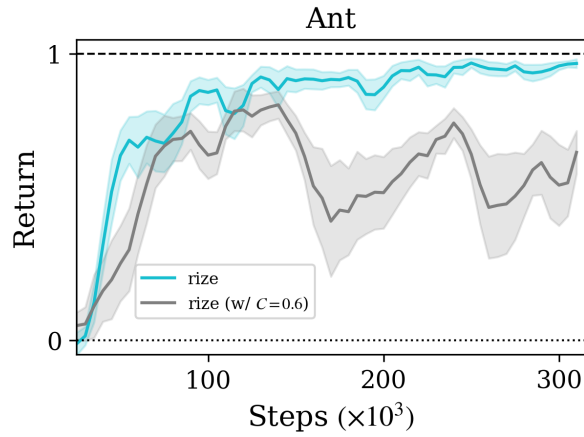


Figure 9: Fine-tuning of the regularizer coefficient ( $C$ ). Turquoise shows our method’s primary result with  $C = 0.1$  for Ant-v2, while gray indicates a larger value ( $C = 0.6$ ). Only one parameter is varied at a time, and three trajectories are used throughout the analysis.

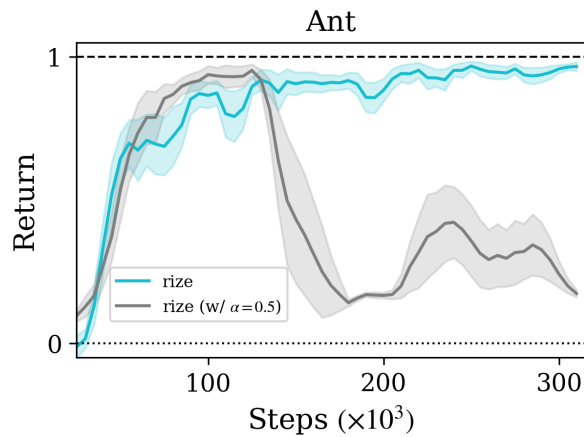


Figure 10: Fine-tuning of the temperature parameter ( $\alpha$ ). Turquoise shows our method’s primary result with  $\alpha = 0.05$  for Ant-v2, while gray indicates a larger value ( $\alpha = 0.5$ ). Only one parameter is varied at a time, and three trajectories are used throughout the analysis.